Full Paper

CSIRO PUBLISHING

Aust. J. Chem. **2011**, *64*, 1366–1372

www.publish.csiro.au/journals/ajc

2-Chloro-2,2-difluoracetamide ($ClF_2CC(O)NH_2$). Thermal Decomposition, Vapour Infrared, Mass Spectrometry, Low-temperature NMR, and Theoretical Studies. Solvent Effects on Conformational Preferences

Ana G. Iriarte,[A] *Edgardo H. Cutin,*[B] *and Gustavo A. Argüello*[A,C]

[A]Instituto de Investigaciones en Físico Química de Córdoba (INFIQC) – Departamento de Fisicoquímica, Facultad de Ciencias Químicas, Universidad Nacional de Córdoba, Ciudad Universitaria, 5000 Córdoba, Argentina.

[B]Instituto de Química del Noroeste Argentino (INQUINOA), Instituto de Química Física, San Lorenzo 456, T4000 CAN Tucumán, Argentina.

[C]Corresponding author. Email: gaac@fcq.unc.edu.ar

Gas-phase thermal decomposition of 2-chloro-2,2-difluoracetamide (CDFA) was studied at temperatures between 270 and 290°C. The rate constant for the decomposition follows the Arrhenius equation.

$$k = (5.5 \pm 0.3) \cdot 10^{16}\ s^{-1} \exp\left[-\frac{(104 \pm 4)\ kJ\ mol^{-1}}{RT}\right]$$

Mass spectrometry was used to analyze the decomposition pattern of the title compound. The FT-IR spectrum of the vapour phase and the infrared spectra of CDFA in protic and aprotic solvents were recorded. Potential energy surfaces were studied by theoretical calculations performed at the density functional theory level (PBEPBE and B3LYP methods) using the 6-31G*, 6-31+G*, 6-311+G**, aug-cc-pVDZ, and aug-cc-pVTZ basis sets.

Manuscript received: 24 August 2010.
Manuscript accepted: 30 May 2011.
Published online: 23 August 2011.

Introduction

Amide compounds are well known as peptide analogues, and as such, they could help provide relevant information about the conformation of proteins.[1–14] A large number of experiments have been carried out in order to acquire experimental data related to amide compounds and to reach a better understanding of the different effects that help in the stabilization of these species in different media.[9–16]

However, as far as we know, there is little information about other properties of acetamide derivatives, such as, for instance, the kinetics of thermal or photochemical decomposition. Only a few studies of acetamide photolysis and pyrolysis mechanism have been carried out and their products analyzed.[17,18] In contrast, there are more data about the behaviour of acetamide derivatives in solution. For example, the study of conformational equilibria of *N*,*N*-dimethyl-2-haloacetamides,[9–12] *N*-methyl-2-fluoroacetamide[10] and fluoro-, chloro-, bromo-, and cyano-acetamide[11,12] deals with the presence of at least two stable rotamers in some solvent systems. Also, the infrared spectra of compounds such as formamide, *N*-methyl formamide, acetamide, and *N*-methylacetamide show marked shifts of the C=O stretching vibration bands with solvation in both protic and aprotic solvents.[15] In order to study the latter fact in greater depth, Eaton et al.[15] carried out the spectroscopic analysis of some acetamide derivatives in solvents, and investigated the carbonylic band behaviour when increasing concentrations of aprotic solvents were added to methanolic systems. They concluded that, for some methanolic and aqueous systems, there are two kinds of solvates. One type corresponds to monosolvated C=O species, whereas the other is related to the di-hydrogen-bonded C=O compounds. The occurrence of each type depends on the relative concentration of the 'free' O–H groups in the media, i.e. the availability of O–H groups to form hydrogen bonds. In a recent theoretical investigation of the *N*-methylacetamide/methanol system,[19] Kwac et al. concluded that the non-Gaussian profile of the IR band was due to the presence of two different solvated structures.

2-Chloro-2,2-difluoroacetamide (CDFA), which is one of the simplest halogen-substituted amide compounds capable of presenting more than one conformation around the sp^3 carbon atom, became of interest both because of its molecular conformation in the gas phase and its vibrational spectrum in the crystal form.[4,20] For this compound, the vibrational spectra have been investigated by solid-phase IR and Raman techniques, and its structure was solved by gas electron diffraction and quantum chemical calculations.[14,20] Although this compound is frequently used as a chemical precursor,[21–23] neither the gas-phase infrared spectrum nor its thermal decomposition have been reported, and neither experimental nor theoretical studies have been carried out in solution.

10.1071/CH10263

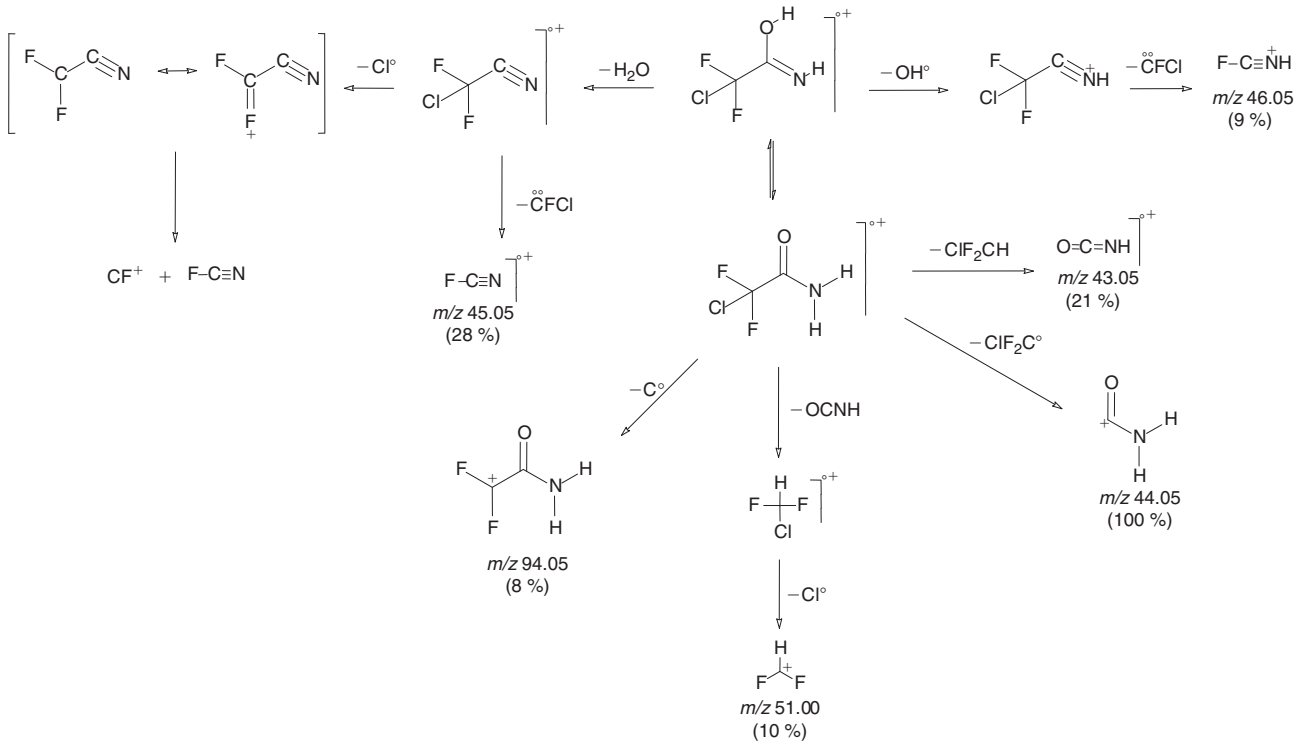

Scheme 1.

In this work, we provide new data to complete information on the physicochemical properties of CDFA. In pursuing that goal, we present the infrared spectrum of the gas phase, the kinetics of its thermal decomposition, low-temperature NMR spectra, the mass decomposition pattern to help understand the decomposition mechanism, and IR spectra in different solvents, such as CH_2Cl_2, $CHCl_3$, CH_3CN, CH_3OH, CH_3CH_2OH, $CH_3(CH_2)_2OH$, $(CH_3)_3COH$, and $(CH_3)_2CHCH_2OH$, together with theoretical analyses. The latter made use of density functional theory (DFT) methods combined with Tomasi's Polarized Continuum Model (PCM), in order to evaluate the influence of the solvent on conformational stability.[24]

Results and Discussion

Analysis of Mass Spectra

Scheme 1 depicts the relevant fragment patterns responsible for the peaks observed in the mass spectra, together with the proposed mechanism to account for them.

A keto–enol equilibrium is postulated as there are H atoms available bonded to the N atom vicinal to the C=O bond. Thus, peaks such as those at *m/z* 46.05 and 45.05 can be explained through the decomposition of the enol form, whereas those peaks at *m/z* 43.05, 44.05, 51.00, and 94.05 could come only from the keto form.

A distinctive feature is the dominant peak of the spectrum, which corresponds to $m/z = 44.05$. Many halogenated acetamides reported in the literature show this peak, and it can be directly assigned to the Csp^3–Csp^2 rupture coming from the carbonylic form. As CDFA has very strong mesomeric delocalization (denoted as $\eta_N \rightarrow \pi^*_{C=O}$),[16] which reinforces the N–Csp^2 bond, the occurrence of the Csp^3–Csp^2 rupture is quite logical.

Infrared Gas-phase Spectra and Thermal Decomposition

We present in Fig. 1 a set of vibrational spectra of CDFA: trace (a), the experimental IR spectrum recorded at 200 °C; trace (b), the calculated IR spectrum and (e), the calculated Raman spectrum, at the B3LYP/6–311++g** level of approach. Traces (c) and (d) correspond to the infrared and Raman spectra respectively reported for the solid.[14] The corresponding wavenumber values are collected in Table 1, in order to facilitate comparison among the different phases, together with the root mean square deviation (RMSD), used to figure out how much the experimental values deviate from the theoretical ones.

The comparison between traces (a) and (b) shows remarkable agreement not only in the position of the bands but also in their intensities. Only a small difference is observed, due to an inversion in the intensities of the bands located at 1171 and 1101 cm^{-1}.

In the amide I and II region (1800–1600 cm^{-1} approximately), there are two distinctive features: the separation of the bands corresponding to the amide I and II modes (from 1734 (solid phase) to 1778 cm^{-1} (gas phase) and from 1690 (solid phase) to 1591 cm^{-1} (gas phase)), and the decrease in the intensity of the NH_2 deformation band, which reaches approximately one-third of the intensity with respect to the original C=O stretching band absorption. This phenomenon is expected to occur, as it has been observed for many primary amides in dilute solutions.[25]

In order to improve the vibrational assignments of the solid,[14] we took advantage of the new information provided by the gas-phase spectrum to verify or to correct the assignments of those bands where the normal modes of vibrations seem to be not well defined. For instance, the band assigned to CF_2 antisymmetric stretching is reported at 1390 cm^{-1} in the solid phase, overlapping with the CN stretching vibration signal (1400 cm^{-1}).[14] As our results fit very well with the calculated

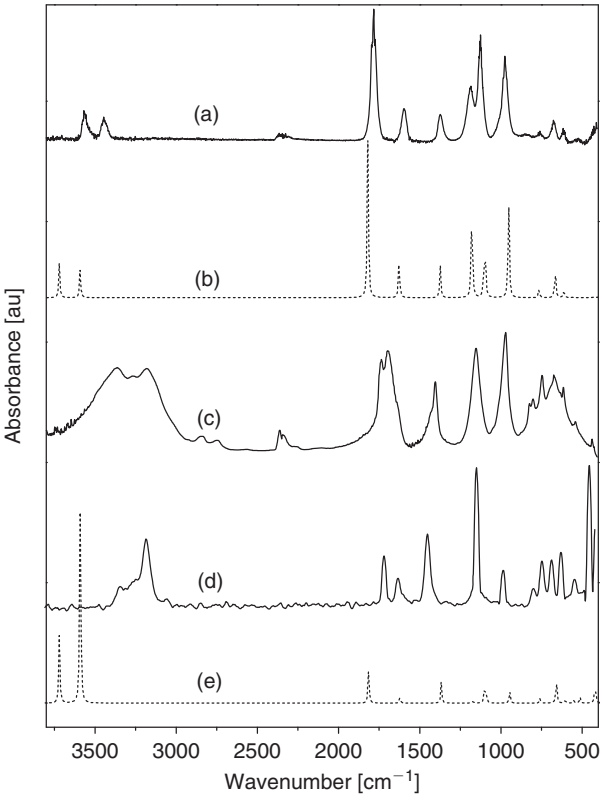

Fig. 1. Infrared and Raman spectra of 2-chloro-2,2-difluoracetamide (CDFA). (a) FT-IR gas phase, 200 °C; (b) and (e) calculated IR and Raman spectra respectively (6–311++g** basis set); (c) FT-IR solid phase; (d) FT-Raman solid phase.

gas-phase spectra, it is logical to assume that the Raman spectra also will. Besides, analysis of the vibrational spectra of molecules containing fluorinated groups such as CF_3 or $CClF_2$ shows a remarkable aspect: they have very intense bands in the infrared, but very weak bands in the Raman spectra.[26] In this context, it is possible to infer that the band located at 1368 cm^{-1} (Raman calculated spectra) does not correspond to a vibration involving the CF_2 group, because that band has an appreciable intensity. Thus, we assigned the CF_2 antisymmetric stretching vibration to the signal located at 1120 cm^{-1} in the gas phase spectra, and re-assigned this vibration mode in the solid to the band at 1146 cm^{-1} (IR).

Other substantial changes could be made using the considerations outlined above. For example, the calculations predicts the CF_2 symmetric and NH_2 deformation modes at 1101 and 1092 cm^{-1} respectively. However, when considering the Raman intensities and the infrared gas-phase experimental spectra, the NH_2 deformation modes could be attributed to the band at a higher wavenumber (1101 cm^{-1}) whereas the CF_2 symmetric mode was attributed to those located at 1092 cm^{-1} (see Table 1).

Continuing the study of CDFA, the thermal decomposition of gaseous CDFA was investigated. The compound, at 2 KPa, was investigated at four different temperatures between 270 and 290 °C. Dry air was allowed to enter the steel reactor at atmospheric pressure, to ensure the rate constant for decomposition was independent of pressure. In addition, in order to examine the role that oxygen or air could be playing in the decomposition, the experiments were performed under an N_2 atmosphere, producing similar results.

The disappearance of the reagent was followed using FT-IR spectroscopy by considering the C=O stretching vibration band

Table 1. Normal modes of vibration, approximate description and infrared and Raman spectra of 2-chloro-2,2-difluoracetamide (CDFA)

Mode	Approximate description[B]	B3LYP/6–311++G** [cm^{-1}][A]	Gas IR [cm^{-1}][C]	Solid IR [cm^{-1}][A]	Solid Raman [cm^{-1}][A]
ν_1	NH_2 asym. stretch.	3719	3563	3355	3331
ν_2	NH_2 sym. stretch.	3590	3444	3178	3173
ν_3	C=O stretch. (amide I)	1814	1778	1734	1703
ν_4	NH_2 def. (amide II)	1622	1591	1690	1616
ν_5	C–N stretch.	1368	1368	1400	1435
ν_6	CF_2 asym. stretch.	1171	1179	1146	1132
ν_7	NH_2 def.	1101	1120		
ν_8	CF_2 sym. stretch.	1092			1075
ν_9	C–Cl stretch.	949	970	970	969
ν_{10}	C=O def.	759	753	740	781
ν_{11}	C–C stretch.	660	667	668	729
ν_{12}	C=O def.	605	606	609	668
ν_{13}	NH_2 def.	556	–	534	610
ν_{14}	ClF_2C def.	512	–	–	527
ν_{15}	ClF_2C def.	421	–	428	436
ν_{16}	ClF_2C def.	372	–	–	395
ν_{17}	ClF_2C def.	344	–	–	343
ν_{18}	NH_2 def.	332	–	–	279
ν_{19}	CCN def.	259	–	–	210
ν_{20}	Skeletal torsion	189	–	–	160
ν_{21}	ClF_2C torsion	44	–	–	–
	Root mean square deviation	–	65 (20)[D]	158 (40)[D]	

[A]Ref. [14].
[B]Stretch.: stretching; def.: deformation; sym.: symmetric; asym.: antisymmetric.
[C]Present work.
[D]Values derived without the contribution of the N–H stretchings.

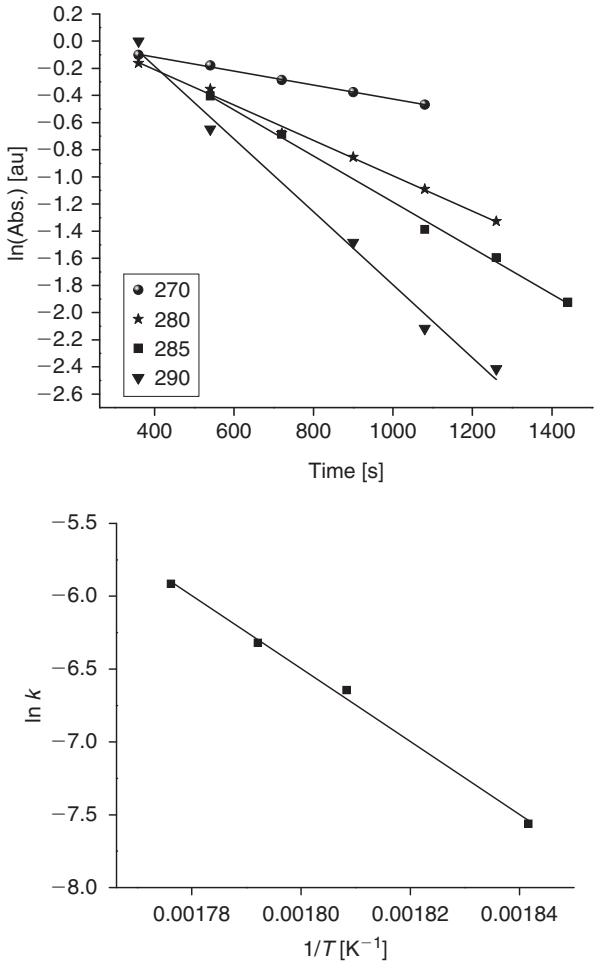

Fig. 2. (Upper) First-order kinetic curves at selected temperatures for the decomposition of 2-chloro-2,2-difluoracetamide (CDFA). (Lower) Arrhenius plot of kinetic data obtained for CDFA.

Table 2. First-order rate constants from the decomposition of 2-chloro-2,2-difluoracetamide (CDFA) at different temperatures

T [°C]	k [s^{-1}]
270	$5.16 \pm 0.12 \times 10^{-4}$
280	$1.30 \pm 0.04 \times 10^{-3}$
285	$1.70 \pm 0.06 \times 10^{-3}$
290	$2.69 \pm 0.14 \times 10^{-3}$

intensity at each temperature. The data were analyzed according to first-order kinetics:

$$-\frac{d[ClF_2CC(O)NH_2]}{dt} = k_{exptl}[ClF_2CC(O)NH_2]$$

Fig. 2 shows the first-order decay at the four temperatures and its associated Arrhenius plot.

Good straight lines are observed in all cases. At each temperature studied, the first-order rate constant was calculated from the plot by a least-squares method. Average rate constants are given in Table 2.

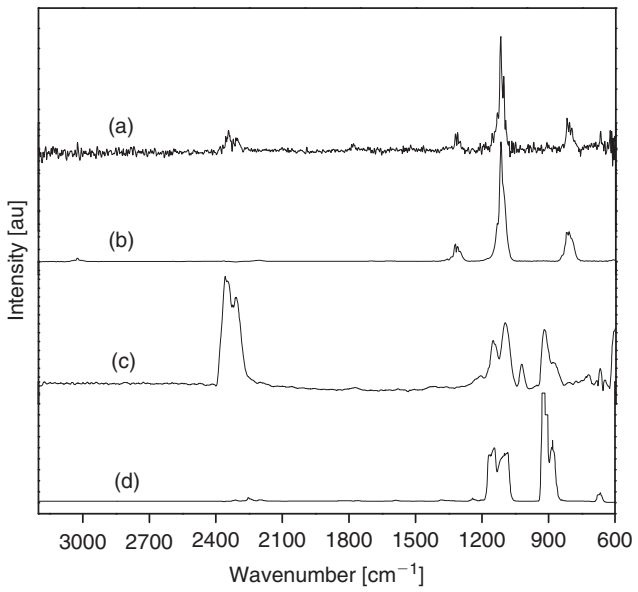

Fig. 3. Gas-phase decomposition product infrared spectra. (a) (Glass + Fe) system product. (b) Reference experimental spectrum of $CHClF_2$. (c) Stainless-steel cell system product. (d) Reference experimental spectrum of CCl_2F_2.

The least-squares analysis of the data from Table 2 gave the following expression for the activation energy:

$$k_{exptl}[CDFA] = (5.5 \pm 0.3) \cdot 10^{16}\ s^{-1} \times \exp\left[-\frac{(104 \pm 4)\ kJ\ mol^{-1}}{RT}\right]$$

Our experimental results fit very well with a first-order kinetic reaction equation, whereas those reported for acetamide and some *N*-substituted acetamides[18,27] conform to a second-order equation. A substantial difference between our results and those reported could arise from the use of the iron reactor. In order to better understand the experimentally observed behaviour, other reactions were tested. In different glass ampoules, CDFA was introduced with and without iron threads and finely divided flat silicon wafers to simulate the whole steel reactor environment. In order to investigate the thermal decomposition, the ampoules were heated at 280°C for 20 min. The corresponding FT-IR spectra of the products were recorded, except for the system without iron threads or silicon wafers as there was no reaction over this period of time. In Fig. 3 are shown the corresponding infrared spectra obtained in both the steel and glass ampoule reactors, together with the spectra of the possible products used as reference.

The IR spectrum of the reaction carried out in the steel reactor (Fig. 3c) shows different bands in comparison with that registered from the glass ampoule/iron threads combination (Fig. 3a). As far as we know, there have been no experimental studies on the nature of the products obtained from the thermal decomposition of the title compound; therefore, we could postulate some products from the signals observed in the infrared spectra. Apart from CO_2, which is the major product (see Fig. 3), it was also possible to observe $CHClF_2$ as the most important product in the glass system (compare with trace (b), which corresponds to pure $CHClF_2$[28]), and CCl_2F_2 (compare with trace (d), which corresponds to pure CCl_2F_2[28]) in the steel reactor.

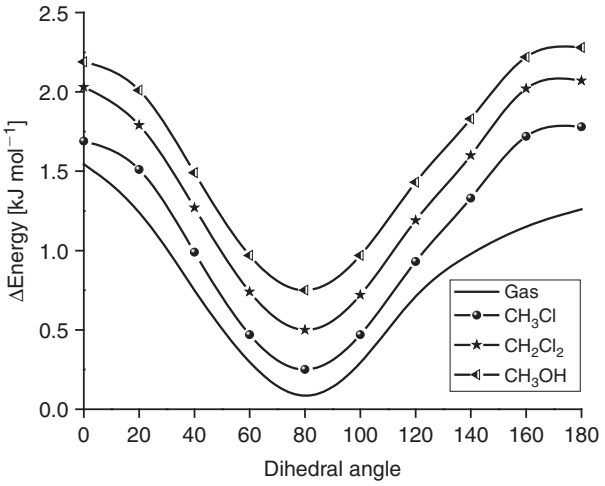

Fig. 4. Potential energy curves calculated at 20 °C steps for different phases, calculated at B3LYP/6–311+G** level or approach. The CH_3Cl, CH_2Cl_2, and CH_3OH curves are shifted by 1, 2, and 3 kJ mol^{-1} from the gas-phase curve respectively.

Infrared and ^{1}H NMR Analysis of CDFA in Solution

There is relevant information about structural conformations and the solvation of amide and haloacetamide derivatives in different solutions, as was mentioned above.[6,10,11,29] Taking into account those results, we carried out experimental and theoretical studies in solution to confirm whether CDFA exists in more than one conformation. Potential energy curves, where the dihedral angle capable of generating other conformers was varied, were obtained using DFT methods with different basis sets (see Computational Method section), using the *Gaussian 03* program.[30] The PCM[24] was included to take into account the solvent effect on rotational isomerism. In Fig. 4, curves corresponding to the gas phase (bottom line) and results calculated in different solvents (CH_3Cl, CH_2Cl_2, and CH_3OH) are presented.

One evident minimum is found corresponding to the *gauche* form, with the angle between the Cl−C bond and the C=O double bond at ~80°. However, with the aim of examining all of the possible configurations, geometry optimizations using standard convergence criteria without symmetry restrictions were carried out. According to the calculations there is no possibility that CDFA exists in other conformations but the *gauche* one, either in the gas phase or in solution. The existence of imaginary frequencies for the *syn* and *anti* conformations in both gas phase and solution support this conclusion (see Fig. S1, Accessory Publication). However, the potential curves obtained from internal rotation around the C–C bond (in solution) show a plateau at (Cl−C–C=O) ≈ 180°, suggesting that some interactions stabilizing this conformation could exist. TCA (trichloroacetamide) and TFA (trifluoroacetamide) in some solvent systems present strong solute–solvent interactions, which have been analyzed by FT-IR.[6] The authors observed that the wavenumber of the C=O bands did not change with concentration, concluding that all the molecules are associated with solvent. In order to verify if this occurred in our system, a series of IR spectra were recorded in CH_3CN at different concentrations of CDFA. The corresponding spectra are given in Fig. S2 of the Accessory Publication, where it is noticeable that the C=O band does not change with concentration either. Thus, it can be presumed that CDFA presents this kind of interaction in solutions.

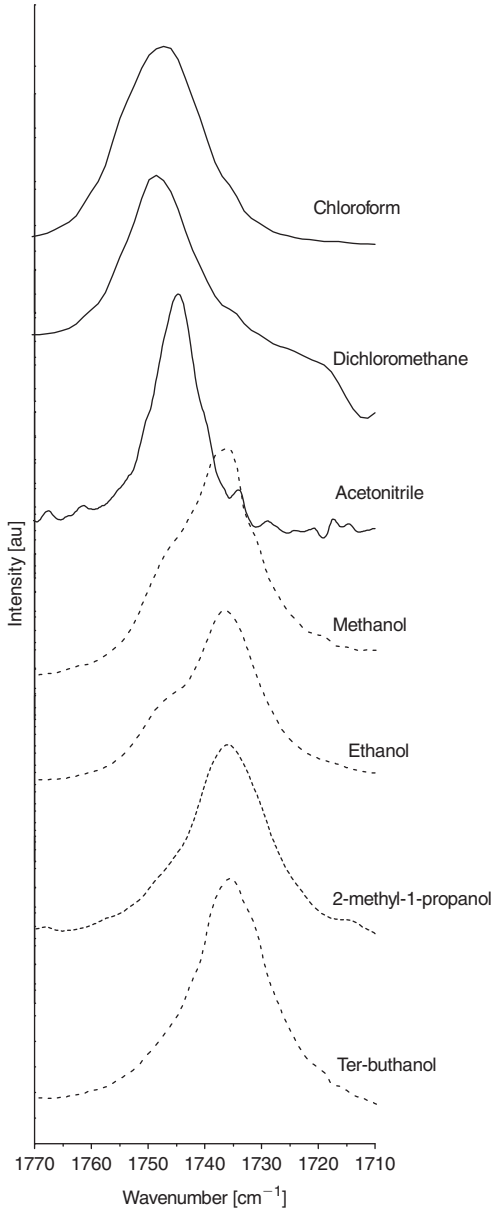

Fig. 5. Spectra of 2-chloro-2,2-difluoracetamide (CDFA) in protic and aprotic solvents, in the region of the carbonyl group band.

Nevertheless, in gas and solid phases, the $CClF_2$ group behaviour is determined by the intramolecular F···H hydrogen bond and by O···F and O···Cl repulsions. In fact, the calculated Cl···H distance in the gas phase (2.51 Å) is shorter than the same distance in solvents (2.57 Å in dichloromethane and 2.58 Å in methanol).

The experimental infrared spectra were recorded for CDFA not only in aprotic solvents (chloroform, dichloromethane, and acetonitrile; Fig. 5) but also in protic ones in order to further investigate the experimental behaviour in solution.

In Fig. 5, the dashed-line traces correspond to CDFA in protic solvents. There are two important points to note: the first one is the shift of C=O bands to lower frequencies as the nature of the solvent changes on going from aprotic to protic, and the second is the splitting of the C=O bands in the CDFA/methanol and CDFA/ethanol systems spectra. The H bridge between the oxygen atom (of the C=O group) and the OH of the protic

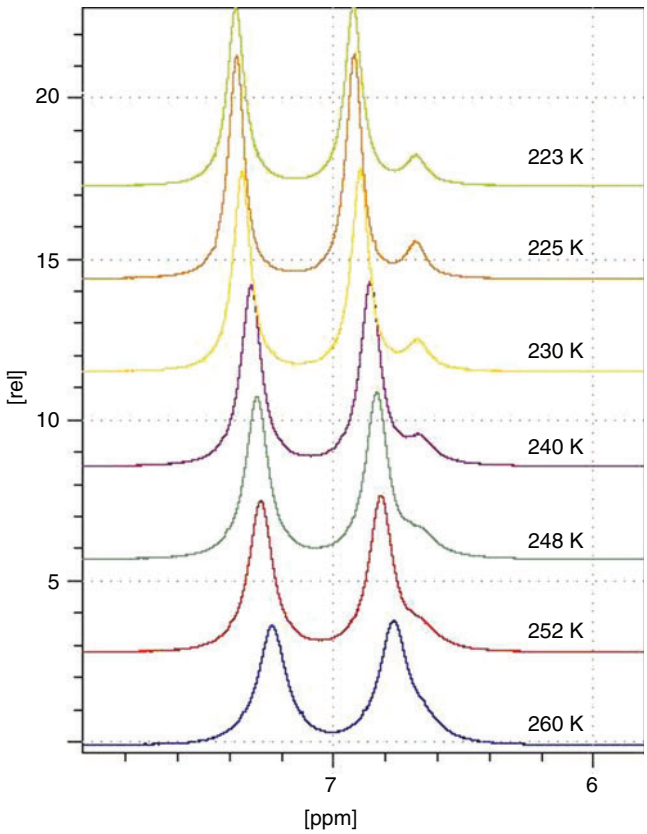

Fig. 6. Low-temperature ^{1}H NMR spectra at different temperatures and with a small amount of water added.

solvent acts to weaken the C=O stretching vibration, causing the band to shift to lower frequencies, as has been clearly observed for acetamide, *N*-methyl acetamide, dimethyl acetamide, etc.[15] In the cases where the solvent is methanol or ethanol, two bands are observed in the C=O region. The band appearing as a shoulder at higher frequencies could be associated with the presence of the non-hydrated population, i.e. with the carbonyl groups not forming hydrogen bonds with the solvent, as revealed by the band position that coincides with the band in aprotic solvents. However, as the existence of a doubly hydrated C=O population in some solvents such as methanol or ethanol has been reported elsewhere,[15,19] we performed additional experiments, recording ^{1}H NMR spectra at seven different temperatures (223, 225, 230, 240, 248, 252, and 260 K) in order to disprove this assumption for CDFA (see Fig. 6).

Apart from the characteristic peaks corresponding to the NH_2 hydrogen atoms (with splitting due to the slower exchange of the H atoms with the media), an extra signal appeared at 6.7 ppm as the temperature decreased. According to existing data,[25] this signal could be assigned to the hydrogen atom (from an OH group) bonded to the oxygen of the C=O group, forming an H bridge. The presence of only one signal rules out the presence of a doubly hydrated C=O population.

Conclusions

CDFA presents a *gauche* conformation in solution, in both protic and aprotic solvents, as determined by FT-IR and theoretical calculations. ^{1}H NMR results suggest the presence of the mono-hydrated carbonyl group only. The thermal decomposition follows first-order kinetics, and the temperature for effective decomposition depends on the use of Fe as catalyst.

Experimental

CDFA was commercially available and its purity was checked by NMR spectroscopy. The gas-phase infrared spectra (resolution 2 cm^{-1}) were recorded at 270, 280, 285, and 290°C with a Bruker IFS-28 FT-IR spectrometer in the range 4000–600 cm^{-1}. For the solutions, the spectra were measured at room temperature in the range 4000–400 cm^{-1}, and at a concentration of 0.02 mol L^{-1} in solvents of different polarity, using an AgCl cell with an optical path of 0.1 mm.

^{1}H NMR spectra were recorded on a Bruker Avance II 400 MHz spectrometer using $CDCl_3$. Chemical shifts are reported in parts per million [ppm] downfield from TMS. Gas chromatography–mass spectrometry (CG/MS) analyses were performed in a Shimadzu CG-MS-QP 5050 spectrometer equipped with a VF column, using helium as eluent at a flow rate of 1.1 mL min^{-1} and a heating ramp of 25°C min^{-1} from 100° to 280°C. Mass spectra were obtained in electron-impact mode (EI) with 70-eV ionization energy.

The gas-phase IR spectra were taken with a 10-cm-length home-made stainless steel cell with Si windows at each end. The steel reactor was surrounded with electrical tape and the temperature was controlled with a thermocouple.

Computational Methods

Theoretical calculations were performed with *GAUSSIAN 03*,[30] using DFT methods with 6-31G*, 6-31+G*, 6-311+G**, aug-cc-pVDZ, and aug-cc-pVTZ basis sets.

Accessory Publication

The following material is available online on the Journal's website: calculated frequencies for *syn*, *anti*, and *gauche* conformers (Fig. S1a, b, and c respectively) and infrared spectra of the C=O stretching band in acetonitrile solutions from 4.7×10^{-4} to 2.1×10^{-3} M (Fig. S2).

Acknowledgements

Financial support from CONICET, SECYT-UNC, and FONCYT is gratefully acknowledged. A.G.I. thanks Professor Claúdio Tórmena.

References

[1] S. Samdal, R. Seip, *J. Mol. Struct.* **1997**, *413–414*, 423. doi:10.1016/S0022-2860(97)00018-5
[2] S. Gundersen, S. Samdal, R. Seip, D. J. Shorokhov, T. G Strand, *J. Mol. Struct.* **1998**, *445*, 229. doi:10.1016/S0022-2860(97)00427-4
[3] S. Gundersen, S. Samdal, R. Seip, D. J. Shorokhov, *J. Mol. Struct.* **1999**, *477*, 225. doi:10.1016/S0022-2860(98)00617-6
[4] S. Gundersen, V. P. Novikov, S. Samdal, R. Seip, D. J. Shorokhov, V. A. Sipachev, *J. Mol. Struct.* **1999**, *485–486*, 97. doi:10.1016/S0022-2860(99)00088-5
[5] S. Gundersen, S. Samdal, R. Seip, T. G. Strand, *J. Mol. Struct.* **2004**, *691*, 149. doi:10.1016/J.MOLSTRUC.2003.11.039
[6] E. Sánchez de la Blanca, M. V. García, *Spectrochim. Acta A Mol. Biomol. Spectrosc.* **1994**, *50*, 41. doi:10.1016/0584-8539(94)80113-4
[7] K. M. Marstokk, H. Møllendal, S. Samdal, R. Seip, *J. Mol. Struct.* **1996**, *376*, 11. doi:10.1016/0022-2860(95)09045-2
[8] I. G. Binev, B. A. Stamboliyska, Y. I. Binev, *Spectrochim. Acta A Mol. Biomol. Spectrosc.* **1998**, *54*, 843. doi:10.1016/S1386-1425(98)00008-0
[9] P. R. Olivato, S. A. Guerrero, M. H. Yreijo, R. Rittner, C. F. Tormena, *J. Mol. Struct.* **2002**, *607*, 87. doi:10.1016/S0022-2860(01)00761-X

[10] C. F. Tormena, N. S. Amadeu, R. Rittner, R. J. Abraham, *J. Chem. Soc., Perkin Trans. 2* **2002**, 773. doi:10.1039/B111048A
[11] C. R. Martins, R. Rittner, C. F. Tormena, *J. Molec. Struct. THEO.* **2005**, *728*, 79. doi:10.1016/J.THEOCHEM.2005.04.033
[12] H. Møllendal, S. Samdal, *J. Phys. Chem. A* **2006**, *110*, 2139. doi:10.1021/JP056598K
[13] S. Pedersoli, C. F. Tormena, R. Rittner, *J. Mol. Struct.* **2008**, *875*, 235. doi:10.1016/J.MOLSTRUC.2007.04.037
[14] A. G. Iriarte, E. H. Cutin, C. O. D. Védova, *J. Mol. Struct.* **2006**, *800*, 154. doi:10.1016/J.MOLSTRUC.2006.04.009
[15] G. Eaton, M. C. R. Symons, P. P. Rastogi, *J. Chem. Soc., Faraday Trans. I* **1989**, *85*, 3257. doi:10.1039/F19898503257
[16] G. Eaton, M. C. R. Symons, P. P. Rastogi, W. E. W. Colm O'Duinn, *J. Chem. Soc., Faraday Trans.* **1992**, *88*, 1137. doi:10.1039/FT9928801137
[17] B. C. Spall, E. W. R. Steacie, in *Proceedings of the Royal Society of London, Vol. 239*, Series A. Mathematical and Physical Sciences, **1957**, p. 1 (Royal Society of London: London).
[18] J. Aspden, A. Maccoll, R. A. Ross, *Trans. Faraday Soc.* **1968**, *64*, 965. doi:10.1039/TF9686400965
[19] K. Kwac, H. Lee, M. Cho, *J. Chem. Phys.* **2004**, *120*, 1477. doi:10.1063/1.1633549
[20] B. Kalyanaraman, L. D. Kispert, J. L. Atwood, *J. Cryst. Mol. Struct.* **1976**, *6*, 311. doi:10.1007/BF01292368
[21] N. Nakajima, M. Saito, M. Ubukata, *Tetrahedron* **2002**, *58*, 3561. doi:10.1016/S0040-4020(02)00304-6
[22] N. Nakajima, M. Saito, M. Kudo, M. Ubukata, *Tetrahedron* **2002**, *58*, 3579. doi:10.1016/S0040-4020(02)00305-8
[23] Y. Takano, H. Tanaka, K. Takano, Y. Hashimoto, in *European Patent Application* **2000**.
[24] S. Miertuš, E. Scrocco, J. Tomasi, *Chem. Phys.* **1981**, *55*, 117. doi:10.1016/0301-0104(81)85090-2
[25] R. M. Silverstein, G. C. Bassler, T. C. Morrill, *Spectrometric Identification of Organic Compounds, 4th edn* **1981** (John Wiley & Sons: New York, NY).
[26] A. G. Iriarte, *Ph.D. Thesis: Caracterización estructural y vibracional de compuestos con enlace fosforo nitrógeno* **2007**, Universidad Nacional de Tucumán, Argentina.
[27] A. Maccoll, S. S. Nagra, *J. Chem. Soc. Faraday Trans. 2* **1974**.
[28] S. E. Stein, in *NIST Mass Spec Data Center* **2010** (Eds P. J. Linstrom, W. G. Mallard) (National Institute of Standards and Technology: Gaithersburg, MD).
[29] P. R. Olivato, S. A. Guerrero, M. H. Yreijo, R. Rittner, C. F. Tórmena, *J. Mol. Struct.* **2002**, *607*, 87.
[30] M. J. Frisch, G. W. Trucks, H. B. Schlegel, G. E. Scuseria, M. A. Robb, J. R. Cheeseman, J. A. J. Montgomery, T. Vreven, K. N. Kudin, J. C. Burant, J. M. Millam, S. S. Iyengar, J. Tomasi, V. Barone, B. Mennucci, M. Cossi, G. Scalmani, N. Rega, G. A. Petersson, H. Nakatsuji, M. Hada, M. Ehara, K. Toyota, R. Fukuda, J. Hasegawa, M. Ishida, T. Nakajima, Y. Honda, O. Kitao, H. Nakai, M. Klene, X. Li, J. E. Knox, H. P. Hratchian, J. B. Cross, C. Adamo, J. Jaramillo, R. Gomperts, R. E. Stratmann, O. Yazyev, A. J. Austin, R. Cammi, C. Pomelli, J. W. Ochterski, P. Y. Ayala, K. Morokuma, G. A. Voth, P. Salvador, J. J. Dannenberg, V. G. Zakrzewski, S. Dapprich, A. D. Daniels, M. C. Strain, O. Farkas, D. K. Malick, A. D. Rabuck, K. Raghavachari, J. B. Foresman, J. V. Ortiz, Q. Cui, A. G. Baboul, S. Clifford, J. Cioslowski, B. B. Stefanov, G. Liu, A. Liashenko, P. Piskorz, I. Komaromi, R. L. Martin, D. J. Fox, T. Keith, M. A. Al-Laham, C. Y. Peng, A. Nanayakkara, M. Challacombe, P. M. W. Gill, B. Johnson, W. Chen, M. W. Wong, C. Gonzalez, J. A. Pople, *Gaussian Revision C 02.* **2004** (Gaussian, Inc.: Wallingford, CT).